A Generic Incompressible Smoothed Particle Galerkin Framework for Modeling and Optimization of Thermal Interface Material and Adhesive Spreading

Henan Mao, Junyan He, Sameer Jape, Yi Zhang, Xiaofei Pan
Synopsys, Inc
675 Almanor Ave
Sunnyvale, CA 94085 US
Email: hemao@synopsys.com

Abstract

Modern electronics packaging and consumer electronics assembly increasingly rely on precisely controlled dispensing and compression of highly viscous polymer materials, including thermal interface materials (TIM) and structural adhesives. In thermal management applications, insufficient TIM spreading can create air voids and nonuniform bond-line thicknesses that increase thermal resistance and compromise device reliability, while in adhesive bonding applications incomplete coverage or overflow can degrade mechanical strength, sealing performance, and manufacturability. Despite their different functional roles, these processes share the same underlying physics: large-deformation squeeze flow of viscous and often non-Newtonian fluids with evolving free surfaces, moving contact boundaries, wetting effects, and possible void entrapment. This paper presents a generic computational framework based on the Incompressible Smoothed Particle Galerkin method for simulating and optimizing TIM and adhesive spreading processes. The proposed Lagrangian meshfree formulation solves the incompressible flow problem while naturally accommodating severe free-surface deformation and the merging of multiple fluid fronts without the mesh distortion challenges associated with conventional mesh-based CFD approaches. Rheological effects such as shear-thinning viscosity, as well as surface tension and wall adhesion effects, are incorporated to capture realistic material behavior. A systematic design-of-experiments study is performed to evaluate the influence of dispensing pattern geometry, dispensed volume, and final bond-line thickness on coverage quality, overflow tendency, and void formation. The results demonstrate that the framework can efficiently construct a virtual process window for dispensing design, enabling early-stage optimization before physical prototyping. By providing physics-based insight into spreading morphology and defect formation, the proposed ISPG framework offers a versatile simulation tool for improving material coverage, reducing experimental trial-and-error, and accelerating process development across semiconductor packaging and electronics assembly applications.

Key words

Thermal interface material; adhesive dispensing; incompressible smoothed particle Galerkin; squeeze flow; electronics packaging

I. Introduction

The continued miniaturization and increasing power density of modern electronic systems have created growing demand for reliable material dispensing processes in both advanced semiconductor packaging and consumer electronics assembly. In thermal management applications, thermal interface materials (TIMs) are dispensed and compressed between heat-generating components and heat spreaders to reduce contact resistance and improve heat dissipation. However, incomplete spreading, nonuniform bond-line thickness, and trapped air voids can significantly degrade thermal performance and device reliability. Previous studies have investigated TIM squeeze-flow behavior, bond-line thickness evolution, and process-dependent material redistribution, highlighting the importance of physics-based modeling for process optimization [1–3].

Similar challenges exist in adhesive bonding processes, where highly viscous polymer adhesives are dispensed to bond, seal, and reinforce electronic components such as battery modules, camera housings, and structural frames. The final adhesive coverage depends strongly on the initial dispensing pattern, compressed gap height, material volume, and rheological properties. Prior work on adhesive compression flow has shown that shear-rate-dependent viscosity, trapped air, and edge overflow are critical factors in determining joint quality [4–6]. Although TIM spreading

and adhesive bonding serve different functional purposes, both processes are governed by large-deformation squeeze flow of viscous, often non-Newtonian fluids with evolving free surfaces and moving contact boundaries.

Numerical simulation provides an effective way to reduce trial-and-error testing, accelerate process development, and connect manufacturing parameters with downstream reliability performance. In electronic packaging, advanced computational workflows have been increasingly used to model solder reflow and free-surface reflow behavior [7,8], board-level drop response [9], and package-level shock and vibration behavior [10]. These studies demonstrate that process-aware and multi-scale simulation methods can provide valuable insight into reliability-critical deformation, stress transfer, and failure mechanisms in complex electronic assemblies [7–10]. However, conventional mesh-based CFD approaches may suffer from mesh distortion or remeshing difficulties when applied to extreme free-surface deformation, thin-gap spreading, and the merging of multiple fluid fronts. Meshfree Lagrangian particle methods, including the Incompressible Smoothed Particle Galerkin method, provide an attractive alternative for incompressible free-surface flows and have been applied to electronic packaging reflow problems involving surface tension and wall adhesion effects [8,11].

This paper presents a generic ISPG-based computational framework for modeling and optimizing TIM/adhesive material spreading processes. In this paper, "TIM/adhesive material" is used as a unified term for thermal interface materials and structural adhesives considered in the dispensing and compression examples. The framework captures large-deformation viscous flow, free-surface evolution, fluid-front merging, shear-thinning behavior, surface tension, and wall adhesion within a unified formulation. A design-of-experiments study is conducted to evaluate the effects of dispensing pattern, material volume, and final bond-line thickness on coverage quality, overflow, and void formation. The proposed method enables construction of a virtual process window for dispensing design and provides practical guidance for reducing physical prototyping, improving material coverage, and supporting reliability-driven process optimization in modern electronics manufacturing.

II. Methodology

To model the compression-driven spreading of thermal interface materials and structural adhesives, the Incompressible Smoothed Particle Galerkin (ISPG) method is adopted in this study. ISPG is a Lagrangian meshfree formulation for incompressible free-surface flow and is suitable for problems involving large material deformation, moving contact boundaries, and evolving free surfaces. A fully implicit solution scheme is used to improve numerical stability and enable larger time increments, while node-cloud-based adaptivity is applied to maintain a uniform particle distribution during severe spreading deformation [8,11,12].

The dispensed material is modeled as an incompressible viscous fluid. At the material–air interface, surface tension introduces a curvature-dependent pressure jump,

$$\sigma_\kappa^{\mathrm{fs}} = \gamma\kappa \tag{1}$$

where γ is the surface tension coefficient and $\kappa = -\nabla \cdot \boldsymbol{n}$ is the mean curvature of the free surface. The pressure boundary condition at the free surface is then written as

$$p^{\mathrm{fs}} = p^{\mathrm{air}} + \sigma_\kappa^{\mathrm{fs}} \tag{2}$$

where p^{air}denotes the surrounding air pressure. This treatment accounts for capillary effects associated with the evolving free surface during spreading. Wall adhesion is modeled through an equilibrium contact angle condition. When the material front contacts a solid wall, the free-surface normal at the wall-contact point is defined as

$$\boldsymbol{n}(\boldsymbol{x}_{\mathrm{w}}) = \boldsymbol{n}_{\mathrm{w}}\cos\left(\theta_{\mathrm{eq}}\right) + \boldsymbol{t}_{\mathrm{w}}\sin\left(\theta_{\mathrm{eq}}\right) \tag{3}$$

where $\boldsymbol{x}_{\mathrm{w}}$ is the wall-contact point, $\boldsymbol{n}_{\mathrm{w}}$ and $\boldsymbol{t}_{\mathrm{w}}$ are the wall-normal and wall-tangential directions, respectively, and θ_{eq} is the prescribed equilibrium contact angle. This boundary treatment enables the model to capture wetting-driven interface evolution during TIM and adhesive spreading.

The above ISPG formulation provides the numerical basis for simulating compression-driven spreading of TIM/adhesive materials with evolving free surfaces, surface tension, and wall-adhesion effects. The following section applies this formulation to a parameterized dispensing model and evaluates the influence of key geometry and process variables through a DOE study.

III. Model Setup, DOE Results, and Sensitivity Analysis

The proposed ISPG formulation was applied to a cross-shaped TIM/adhesive material dispensing pattern compressed between two rigid plates. The objective of the design-of-experiments (DOE) study was to quantify how geometry and process parameters affect the final area coverage ratio after compression. The initial dispensing pattern is parameterized by the center radius, material thickness, angle between adjacent legs, and final gap. During the simulation, the upper plate moves in the normal direction until the prescribed final bond-line thickness, or final gap, is reached. This setup provides a generalized representation of TIM/adhesive material compression and bonding processes commonly encountered in electronic assembly.

The initial geometry is shown in Fig. 1, and the corresponding parameter values are listed in Table 1. The surface tension of the TIM/adhesive material is set to 50 mN/m, and the dynamic viscosity is 20 Pa·s. The contact angle is assumed to be 25° on both the upper and lower surfaces.

TABLE 1: MODEL PARAMETERS

Parameter	Values
Final gap (mm)	0.05, 0.10, 0.15
Glue thickness (mm)	0.17, 0.27
Glue center radius (mm)	0.62, 0.72, 0.82
Angle between legs (°)	20, 45, 70

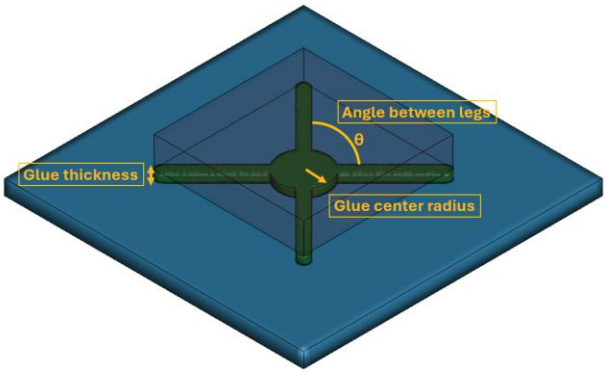


FIGURE 1: PARAMETER DEFINITION OF TIM/ADHESIVE DISPENSING GEOMETRY

A design-of-experiments study was conducted to quantify how dispensing-pattern geometry and compression conditions affect the final spreading morphology. The DOE is structured around key controllable parameters, including center radius, material thickness, angle between adjacent legs, and final gap. For the cross-shaped dispensing pattern, the center radius and leg geometry govern the initial material distribution, while the angle between adjacent legs affects directional spreading uniformity during compression. For each design point, the simulation setup follows the automated workflow illustrated in Fig. 2. All simulation steps are executed using Ansys optiSLang until all prescribed DOE design combinations are completed.

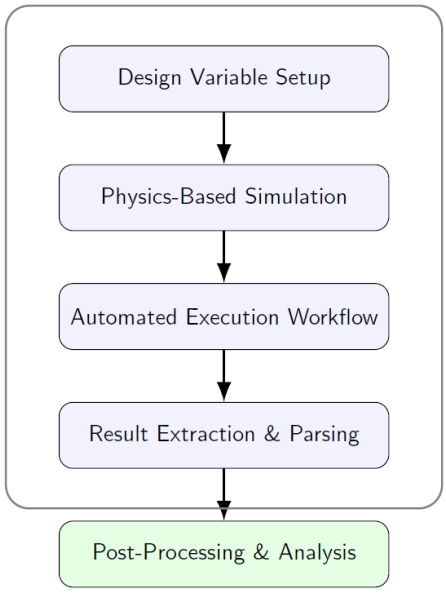


FIGURE 2: DESIGN OF EXPERIMENTS WORKFLOW

The area coverage ratio is defined as the percentage of the target bonding area covered by the TIM/adhesive material after compression to the prescribed final gap. This metric is used as the primary response variable for evaluating DOE performance and comparing different dispensing designs.

After completing the DOE simulations, the resulting coverage responses were analyzed to determine the relative importance of each design parameter. The following section summarizes the main-effect trends, sensitivity ranking, and two-factor response behavior for the TIM/adhesive material spreading process.

The DOE sensitivity ranking in Fig. 3 shows that the final gap is the most dominant factor controlling the area coverage ratio. Its main-effect range reaches 52.0 percentage points, which is much larger than the effect of the other parameters. Material thickness is the second most important factor, with an effect range of 19.0 percentage points. In comparison, center radius and angle between legs show much smaller effects, with ranges of 5.1 and 0.7 percentage points, respectively. This indicates that the global compression condition and available material volume dominate the spreading behavior, while the detailed dispensing-pattern geometry mainly provides secondary tuning.

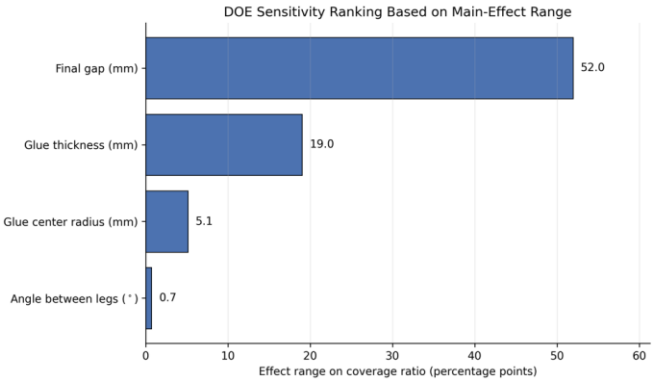


FIGURE 3: SENSITIVITY RANKING BASED ON MAIN-EFFECT RANGE

The normalized sensitivity contribution in Fig. 4 shows the same trend. The final gap contributes 67.6% of the total DOE sensitivity, making it the primary design parameter for improving coverage. Material thickness contributes 24.8%, confirming that the initial material volume strongly affects the final spreading area. The contributions from center radius and angle between legs are only 6.7% and 0.9%, respectively. Therefore, within the investigated design space, coverage optimization should focus first on final gap and material thickness before fine-tuning the center radius and leg angle.

The main-effect plots in Fig. 5 further explain the physical trend of each parameter. As the final gap increases from 0.05 mm to 0.15 mm, the mean coverage ratio decreases significantly, indicating that a smaller gap produces stronger squeeze flow and promotes wider lateral spreading.

Increasing the material thickness from approximately 0.17 mm to 0.27 mm increases the mean coverage ratio because more initial material is available to fill the target region. The center radius also shows a moderate positive effect, while the angle between legs causes only a small non-monotonic change, confirming that the leg angle has limited influence on coverage within the selected DOE range.

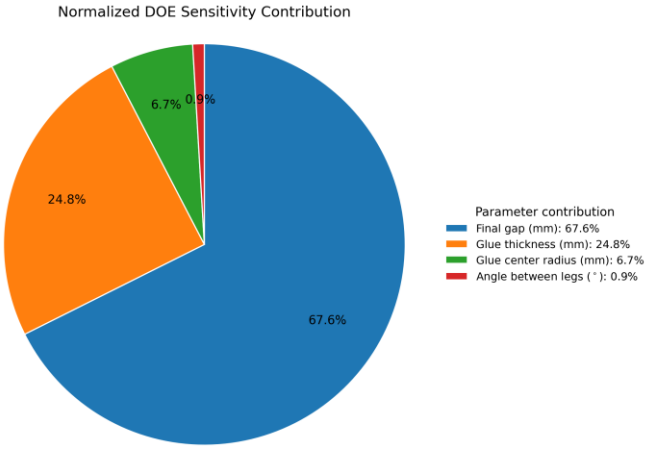
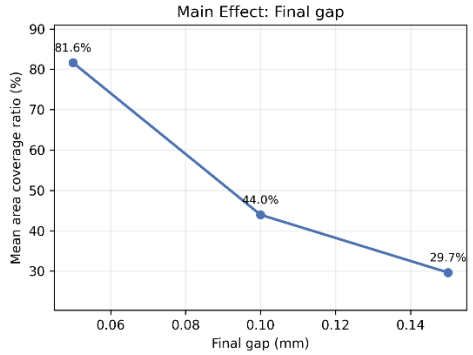
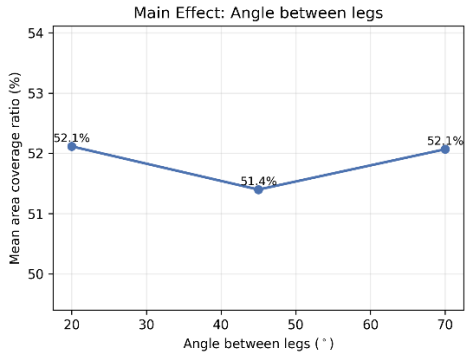


FIGURE 4: NORMALIZED DOE SENSITIVITY CONTRIBUTION

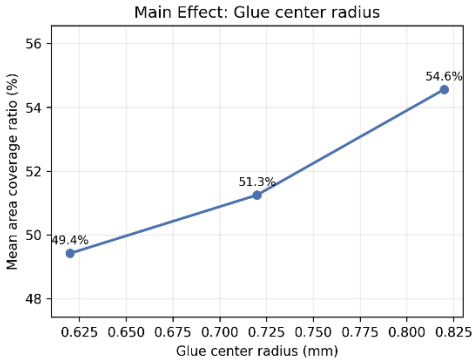
The two-factor response between final gap and material thickness in Fig. 6 highlights the combined effect of compression and material volume. The highest mean coverage ratio is obtained at the smallest final gap and largest material thickness, reaching 95.0% coverage for the case with 0.05 mm final gap and 0.27 mm material thickness. When the final gap increases, the coverage ratio decreases even for the thicker material condition, dropping from 95.0% at 0.05 mm to 53.6% at 0.10 mm and 35.1% at 0.15 mm. For the thinner material case, the same trend is observed, with coverage decreasing from 68.2% to 34.3% and then to 24.2% as the final gap increases. This confirms that final gap has the strongest influence, while material thickness improves coverage but cannot fully compensate for insufficient compression.



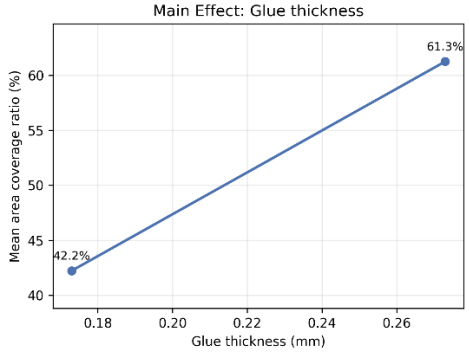
(A)



(B)



(C)



(D)

FIGURE 5: MAIN-EFFECT TRENDS FOR AREA COVERAGE RATIO: (A) FINAL GAP, (B) ANGLE BETWEEN LEGS, (C) CENTER RADIUS, AND (D) ADHESIVE THICKNESS

Overall, the DOE results indicate that the optimal TIM/adhesive dispensing design should prioritize a small final gap and sufficient material thickness to achieve high area coverage. The center radius can be used as a secondary tuning parameter to improve material distribution near the center region; however, its influence is much weaker than that of the final gap and material thickness. The angle between legs shows the lowest sensitivity and is therefore less critical for coverage optimization within the investigated design range. It should be noted that the two-factor response in Fig. 6 represents the mean coverage response averaged over the remaining DOE parameters, while Fig. 7 shows the best individual DOE case. As shown in Fig. 7, the optimal

DOE case, with a final gap of 0.05 mm, a material thickness of 0.27 mm, and a 45° angle between legs, achieves a 100% coverage ratio. This result demonstrates that sufficient initial material volume, combined with strong compression and an optimized dispensing pattern, can fully cover the target area.

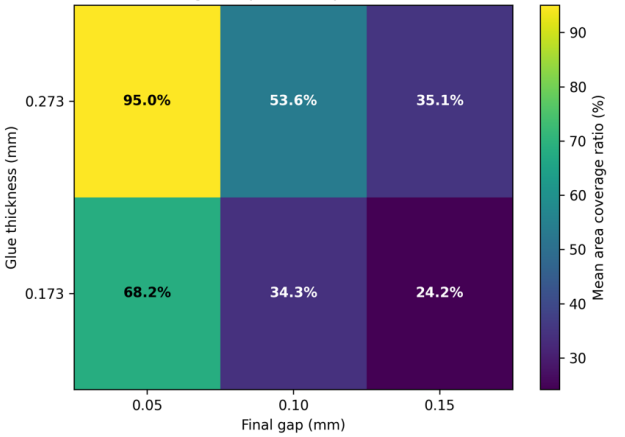


FIGURE 6: TWO-FACTOR RESPONSE OF AREA COVERAGE RATIO FOR FINAL GAP AND ADHESIVE THICKNESS

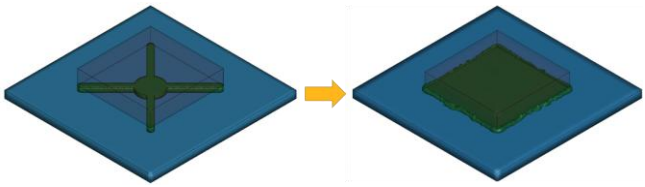


FIGURE 7: FULL ADHESIVE MATERIAL COVERAGE ACHIEVED UNDER THE OPTIMAL DOE DESIGN

IV. Conclusion and Future Work

This study developed an ISPG-based simulation framework for modeling TIM/adhesive material dispensing and compression-driven spreading in electronics assembly applications. The proposed method captures large free-surface deformation, material-front merging, wall adhesion, and squeeze-flow behavior without the mesh distortion challenges typically associated with conventional mesh-based CFD approaches. By combining the ISPG solver with an automated DOE workflow, the framework provides an efficient virtual process development method for evaluating material coverage before physical prototyping.

The DOE results identify final gap as the dominant factor controlling area coverage, followed by material thickness. A smaller final gap enhances spreading by increasing compression-driven flow, while greater material thickness improves coverage by providing more initial volume. In contrast, center radius mainly serves as a secondary tuning parameter for local material distribution, and the angle between legs shows the lowest sensitivity within the investigated design range.

The two-factor response further confirms the coupled effect between final gap and material thickness. The best individual DOE case is obtained with a final gap of 0.05 mm, a material thickness of 0.27 mm, and a 45° angle between legs, achieving a 100% coverage ratio under the optimized design. This result demonstrates that complete target-area coverage can be achieved when sufficient material volume is combined with an appropriate compression gap and dispensing pattern. However, the optimal parameters should still be evaluated together with overflow risk, manufacturing tolerance, and process robustness requirements.

Although the present DOE identifies the dominant design factors, the sampling space remains limited. Future work will refine the optimal process window using a localized response-surface DOE focused on final gap and material thickness, while also considering material-property variations such as viscosity, shear-thinning behavior, surface tension, and contact angle.

References

[1] S. Khalsa and G. Subbarayan, "Squeeze Flow Models for Thermal Interface Materials Contained Between Parallel Plates and Plates With Posts," *Proceedings of the ASME 2011 Pacific Rim Technical Conference and Exhibition on Packaging and Integration of Electronic and Photonic Systems*, Portland, OR, USA, pp. 263–269, 2011.

[2] S. Baeuerle, M. Gebhardt, J. Barth, A. Steimer, and R. Mikut, "Rapid Flow Behavior Modeling of Thermal Interface Materials Using Deep Neural Networks," *arXiv:2208.04045*, 2022.

[3] Purdue University Cooling Technologies Research Center, "Thermal Interface Materials Research," Purdue University, West Lafayette, IN.

[4] M. Müller, J. Finke, L. Stahl, Y. Tong, H. Fricke, and T. Vallée, "Development and Validation of a Compression Flow Model of Non-Newtonian Adhesives," *Journal of Adhesion Science and Technology*, 2021.

[5] S. Ingelsten, A. Mark, R. Kádár, and F. Edelvik, "Simulation of Viscoelastic Squeeze Flows for Adhesive Joining Applications," *Journal of Non-Newtonian Fluid Mechanics*, vol. 300, Article 104722, 2022.

[6] M. Kaufmann, F. Flaig, M. Müller, H. Fricke, and T. Vallée, "Optimized Adhesive Application," *International Journal of Adhesion and Adhesives*, Article 103620, 2024.

[7] H. Mao, J. He, and X. Pan, "A Novel Workflow for Efficient Large BGA Solder Reflow Simulation in Advanced Electronics Packaging," *NAFEMS World Congress*, Salzburg, Austria, 2025.

[8] X. Pan, C. T. Wu, and W. Hu, "Incompressible Smoothed Particle Galerkin Method for an Efficient Simulation of Surface Tension and Wall Adhesion Effects in the 3D Reflow Soldering Process," *Proceedings of the 16th International LS-DYNA Conference*, 2020.

[9] S. Amogh, S. Medikonda, D. Lyu, A. Sengupta, H. Mao, and S. K. M., "Two-Scale Co-Simulation Approach for Drop-Test Simulation of Kovan PCB Board," *Proceedings of the ASME International Mechanical Engineering Congress and Exposition*, vol. 88681, Paper V010T12A034, 2024.

[10] H. Mao, D. Lyu, and T. Zheng, "Advancing Solder Joint Modeling in PCBs: A Two-Scale Co-Simulation Approach for Shock and Vibration Analysis Using LS-DYNA," *Proceedings of the 17th International LS-DYNA Conference*, 2024.

[11] X. Pan, C. T. Wu, and W. Hu, "A Semi-Implicit Stabilized Particle Galerkin Method for Incompressible Free Surface Flow Simulations," *International Journal for Numerical Methods in Engineering*, vol. 121, no. 17, pp. 3979–4002, 2020.

[12] A. Sengupta, X. Pan, D. Lyu, S. Medikonda, A. Shejwal, A. Srivastava, and K. Morgan, "Predicting Solder Shape Evolution During Solder Reflow in Packaging Assembly Processes," *NAFEMS Conference*, 2021.